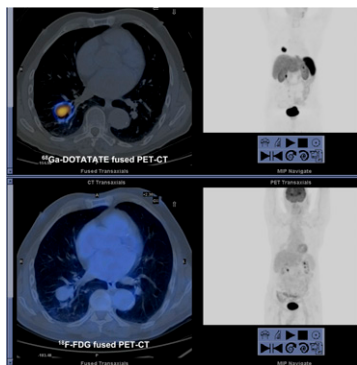


¹⁸F-FDOPA and neuroendocrine tumors: Minn and colleagues provide an overview of the use of this tracer in PET and PET/CT imaging of neuroendocrine tumors, pancreatic β -cell hyperplasia, and other disorders and discuss future applications in diagnosis and therapy. **Page 1915**

Improving lung scintigraphy: Parker previews 2 articles on lung scintigraphy in this issue of *JNM* and reviews the current status of the procedure in the diagnosis of acute pulmonary embolism. **Page 1919**

Nonrigid registration of chest PET/CT: Grgic and colleagues apply intraindividual analysis to determine whether a nonrigid registration algorithm can improve fusion quality of ¹⁸F-FDG PET and CT thoracic images and describe optimal breathing protocols. **Page 1921**

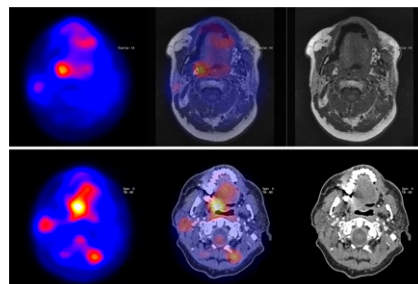
Tracers in pulmonary NET tumors: Kayani and colleagues compare the performance of ⁶⁸Ga-DOTATATE, a novel selective somatostatin receptor 2 ligand, and ¹⁸F-FDG in detection of pulmonary neuroendocrine tumors. **Page 1927**



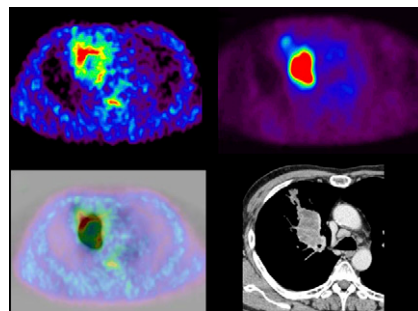
Fitted input function to estimate MR_{glc}: Vriens and colleagues report on and validate a mathematic function to describe the arterial plasma time–activity concentration curve for quantification of glucose metabolic rate and therapy response monitoring with dynamic ¹⁸F-FDG PET. **Page 1933**

¹⁸F-FDG PET in HNSCC follow-up: Krabbe and colleagues assess the role and

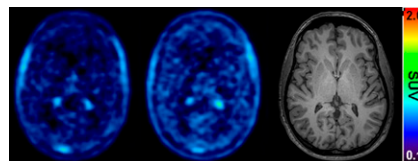
timing of serial ¹⁸F-FDG PET scans as surveillance for early locoregional recurrence, distant metastases, and second primary tumors after treatment for advanced head and neck squamous cell carcinoma. **Page 1940**



¹⁸F-FDG and ⁶²Cu-ATSM in lung cancer: Lohith and colleagues delineate intratumoral uptake and tracer distribution of ⁶²Cu-ATSM, a hypoxic imaging tracer, and ¹⁸F-FDG in patients with lung cancer of pathohistologically different types. **Page 1948**

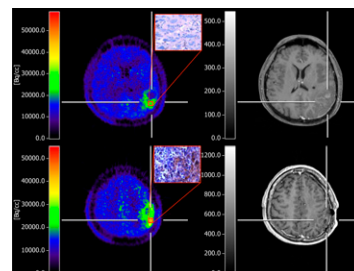


Cerebral P-gp inhibition by tariquidar: Wagner and colleagues use PET with (*R*)-¹¹C-verapamil, a permeability gluco-protein (P-gp) substrate, to measure P-gp function at the human blood–brain barrier after administration of tariquidar, a potent P-gp inhibitor. **Page 1954**

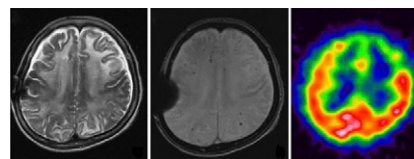


¹¹C-MET PET and glioma progression: Ullrich and colleagues investigate the potential of ¹¹C-MET PET to detect tumor

progression in patients with gliomas and assess changes in tracer uptake and molecular immunohistochemical markers during progression. **Page 1962**



Ischemia in cerebral amyloid angiopathy: Chung and colleagues use ^{99m}Tc-ECD brain perfusion SPECT to characterize cerebral hypoperfusion in patients with cerebral amyloid angiopathy. **Page 1969**



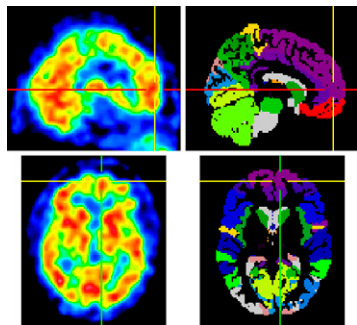
Reference tissue models in BBB disruption: Folkersma and colleagues assess and validate a simplified reference tissue model for analyzing dynamic (*R*)-¹¹C-PK11195 scans in traumatic brain injury, where blood–brain barrier disruptions are likely. . . . **Page 1975**

Endothelial dysfunction in diabetes: Djaberi and colleague explore the diagnostic challenge presented by diabetic patients with myocardial perfusion defects but no evidence of obstructive epicardial coronary disease. **Page 1980**

V/Q SPECT and low-dose CT vs. MDCT in PE: Gutte and colleagues compare the diagnostic abilities of ventilation–perfusion (V/Q) SPECT, V/Q SPECT with low-dose CT, and pulmonary multidetector CT angiography with a combined SPECT/MDCT scanner in pulmonary embolism. **Page 1987**

Cerebral blood flow in diabetes: Káplár and colleagues look for differences in global or regional cerebral blood flow resulting

from microvascular damage in types 1 and 2 diabetes mellitus. **Page 1993**



SPECT for pulmonary embolism: Stein and colleagues provide an educational overview on the current status and accuracy of SPECT in acute pulmonary embolism and discuss its role in the context of increased use of CT angiography. **Page 1999**

Pretargeted RIT of pancreatic cancer: Karacay and colleagues report on a novel pretargeting procedure for therapeutic delivery of ⁹⁰Y-labeled PAM4 IgG, a monoclonal antibody that recognizes a unique epitope associated with a mucin in pancreatic cancer. **Page 2008**

¹⁷⁷Lu-AMBA in GRP-R prostate cancer: Maddalena and colleagues evaluate the tumor binding and imaging potential of this radiolabeled bombesin derivative in low gastrin-releasing peptide receptor models of prostate cancer and determine how reduced expression affects radiotherapeutic efficacy. **Page 2017**

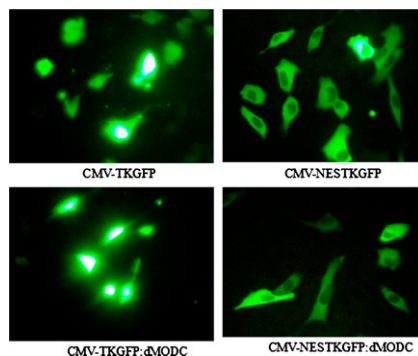
Systemic radionuclide therapy and gliomas: Samnick and colleagues test the therapeutic potential of ¹³¹I-IPA, a tumor-specific amino acid derivative, combined with external-beam photon radiotherapy in glioma-bearing rats. **Page 2025**

RIT with ¹²⁵I-mAbs: Santoro and colleagues assess the in vivo biologic efficiency

of internalizing and noninternalizing ¹²⁵I-labeled monoclonal antibodies for the treatment of small solid tumors. . . . **Page 2033**

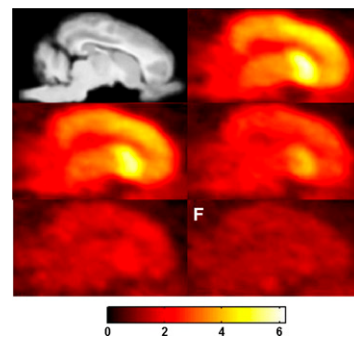
¹⁸F-labeled phosphoramidate: Lapi and colleagues report on studies exploring phosphoramidates as novel small-molecule prostate-specific membrane antigen inhibitors to develop more effective prostate cancer imaging agents with improved specificity and clearance properties. **Page 2042**

Mutant TK/GFP fusion reporter: Hsieh and colleagues construct a mutant thymidine kinase/green fluorescent protein reporter gene with low cytotoxicity and high temporal resolution for real-time optical and PET monitoring of transcription induction and other biochemical changes. . . . **Page 2049**

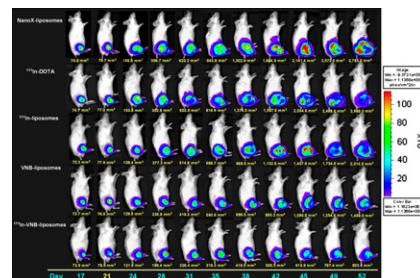


Imaging VEGF receptors in abscesses: Levashova and colleagues determine whether labeled forms of single-chain vascular endothelial growth factor (VEGF) can be used to image VEGF receptors in an animal model of sterile soft-tissue inflammation. **Page 2058**

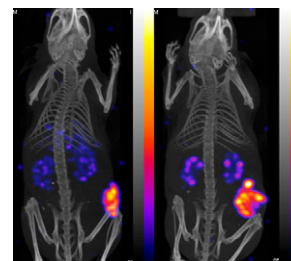
PET radioligand for H₃ receptors: Plisson and colleagues synthesize and evaluate the potential utility of ¹¹C-GSK189254, a histamine H₃ receptor antagonist, for PET imaging of these receptors. . . . **Page 2064**



Therapy and ¹¹¹In-vinorelbine liposomes: Chow and colleagues investigate the therapeutic effectiveness of specific amounts of these PEGylated liposomes by varying radiation dosage and concentrations of chemotherapeutic agents in animal tumor growth suppression studies. . . . **Page 2073**



Radiolabeled divalent gastrin peptide: Sosabowski and colleagues expand on previous studies of ¹¹¹In-labeled divalent gastric peptides with potential for radionuclide therapy in tumors overexpressing gastrin/cholecystokinin subtype 2 receptors. **Page 2082**



ON THE COVER

Both ventilation–perfusion SPECT and multidetector CT angiography have high accuracy in the diagnosis of pulmonary embolism, but only limited data comparing the two are available. A prospective study using a hybrid scanner has concluded that ventilation–perfusion SPECT in combination with unenhanced low-dose CT has excellent diagnostic performance and should probably be considered first-line imaging in the work-up of most cases of pulmonary embolism.

See page 1990.

